Characterization of a CPI-Lexitropsin Conjugate–Oligonucleotide Covalent Complex by ^{1}H NMR and Restrained Molecular Dynamics Simulation

Nancy L. Fregeau,[†] Yuqiang Wang,[†,§] Richard T. Pon,[‡] William A. Wylie,[⊥] and J. William Lown*,[†]

Contribution from the Department of Chemistry, University of Alberta, Edmonton, Alberta, Canada, T6G 2G2, University Core DNA Services, University of Calgary, Calgary, Alberta, Canada T2N 4N1, and Proteus Molecular Design Ltd., Lyme Green Business Park, Macclesfield, Cheshire SK11 0JL, U.K.

Received January 13, 1995[⊗]

Abstract: The structural features of the covalent bonding of a novel CPI-lexitropsin conjugate **4** to a model duplex DNA has been examined by high field ^{1}H-NMR analyses and restrained molecular dynamics calculations. Compound **4**, that was designed for enhanced DNA binding compared with natural (+)CC-1065, exhibits an exceptional cytotoxic potency against KB human nasopharangeal tumor cells *in vitro* of $IC_{50} = 0.76$ fg/L. Racemic **4** reacted readily with the duplex oligodeoxyribonucleotide d(CGCAATTGCG)$_2$ to form a single covalent adduct. The latter exhibits a new absorption band at 396 nm characteristic of the bound drug in addition to the duplex absorption at 258 nm. ^{1}H-NMR analysis confirms by selective chemical shift changes and NOEs between protons in the drug and in the duplex that covalent bonding has taken place at A_4. The drug is aligned in a 5′- to 3′-direction at the AATT core in the minor groove resulting from the selective binding of one enantiomer of **4** and corresponding to the mode of binding of (−)-CC-1065. The stereochemistry at the site of attachment at the 4a position of the drug is (*S*), an inference that is corroborated by the restrained molecular dynamics simulation. The latter computations predict average total energies for the (*R*) and (*S*) drug–DNA adducts of +42 ± 14.36 and -0.42 ± 10.34 kcal/mol, respectively, signifying substantially greater stability for the latter diastereomer. The covalent adduct appears to be quite stable and showed no sign of reversibility such as has been observed with other CPI-based agents which may tentatively be attributed to the exceptionally snug fit of all parts of the drug within the minor groove.

Introduction

Many antitumor compounds exert their bioactivity by targeting DNA. Some, like distamycin A (**1**) and netropsin bind noncovalently to A·T rich regions of DNA in the minor groove. However, covalent binding to DNA usually results in greater cytotoxicity. (+)-CC-1065 (**2**) (Figure 1) is a very potent antitumor antibiotic isolated from *Streptomyces zelensis*.[1] It consists of three substituted pyrroloindole groups (A–C), the first of which is a cyclopropylpyrroloindole (CPI). CC-1065 and its analogs have been shown to bind to the minor groove of DNA and alkylate N-3 of adenine with concomitant opening of the reactive cyclopropyl group and aromatization of the A unit (Scheme 1).[2] Thermal treatment of this covalently modified DNA results in depurination of the alkylated bases followed by strand cleavage, producing a 5′-phosphate and a 3′-modified deoxyribose.[3] Recently, Sugiura, Yamada, and co-workers have determined the exact nature of the products produced from DNA strand cleavage by ptaquiloside, a carcinogenic compound which possesses a reactive cyclopropyl ring which alkylates the N-3 position of purines in an analogous fashion to **2**.[4] (+)-CC-1065 has been shown to preferentially alkylate 5′-PuNTTA* and 5′-AAAAA* sites (Pu = purine, N = any nucleotide, A* = site of alkylation) with the majority of the molecule oriented to the 5′ side of the alkylation site.[3]

The A (CPI) subunit alone can alkylate DNA in a similar manner, but it does not show as great a sequence selectivity.[5,6] Studies of **2** and its analogs have shown that the B and C subunits increase the binding to DNA and the selectivity of alkylation.[5,6] They also affect the ability of these compounds to cause delayed death. Oral administration of those analogs with the same stereochemistry and complete carbon skeleton of **2** resulted in delayed hepatotoxicity in mice at therapeutic doses.[1,5]

Recent studies have shown that many analogs of **2** reversibly alkylate DNA.[7–9] However, **2** itself appears to irreversibly alkylate DNA under the conditions tested. This difference is attributed to the strong noncovalent binding of **2** which either

[†] University of Alberta.
[‡] University of Calgary.
[⊥] Proteus Molecular Design Ltd.
[§] Present address: Palo Alto Institute of Molecular Medicine, 2462 Wyandotte Street, Mountain View, CA 94043.
* To whom correspondence should be addressed. Tel. (403) 492-3646; Fax: (403) 492-8231.
[⊗] Abstract published in *Advance ACS Abstracts,* July 15, 1995.

(1) Reynolds, V. L.; McGovren, J. P.; Hurley, L. H. *J. Antibiot.* **1986**, *39*, 319–334.
(2) Scahill, T. A.; Jensen, R. M.; Swenson, D. H.; Hatzenbuhler, N. T.; Petzold, G.; Wierenga, W.; Brahme, N. D. *Biochemistry* **1990**, *29*, 2852–2860.
(3) Reynolds, V. L.; Molineux, I. J.; Kaplan, D. J.; Swenson, D. H.; Hurley, L. H. *Biochemistry* **1985**, *24*, 6228–6237.
(4) Kushida, T.; Uesugi, M.; Sugiura, Y.; Kigoshi, H.; Tanaka, H.; Hirokawa, J.; Ojika, M.; Yamada, K. *J. Am. Chem. Soc.* **1994**, *116*, 479–486.
(5) Hurley, L. H.; Warpehoski, M. A.; Lee, C.-S.; McGovren, J. P.; Scahill, T. A.; Kelly, R. C.; Mitchell, M. A.; Wicnienski., N. A.; Gebhard, I.; Johnson, P. D.; Bradford, V. S. *J. Am. Chem. Soc.* **1990**, *112*, 4633–4649.
(6) Boger, D. L.; Coleman, R. S.; Invergo, B. J.; Sakya, S. M.; Ishizaki, T.; Munk, S. A.; Zarrinmayeh, H.; Kitos, P. A.; Thompson, S. C. *J. Am. Chem. Soc.* **1990**, *112*, 4623–4632.
(7) Boger, D. L.; Johnson, D. S.; Yun, W. *J. Am. Chem. Soc.* **1994**, *116*, 1635–1656.
(8) Boger, D. L.; Yun, W. *J. Am. Chem. Soc.* **1993**, *115*, 9872–9873.
(9) Warpehoski, M. A.; Harper, D. E.; Mitchell, M. A.; Monroe, T. J. *Biochemistry* **1992**, *31*, 2502–2508.

0002-7863/95/1517-8917$09.00/0

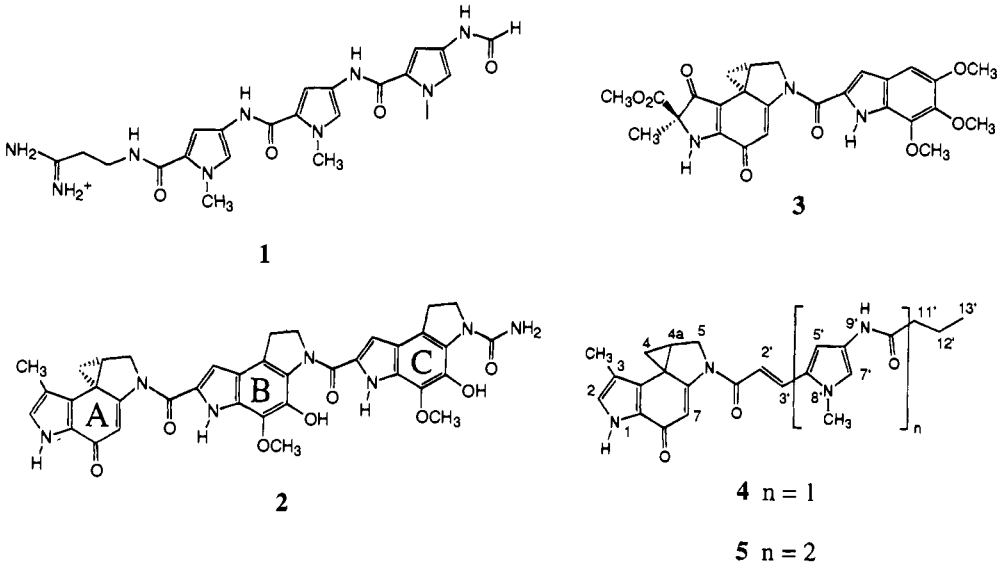

Figure 1. Structures of netropsin **1**; CC-1065 **2**; duocarmycin **3**; and novel CPI-lexitropsin conjugates **4** and **5**.

Scheme 1. Representation of Key Steps Involved in the Covalent Binding of CPI-Based Agents to Adenine-N-3 within the Minor Groove of Duplex DNA and Subsequent Thermally Induced Cleavage

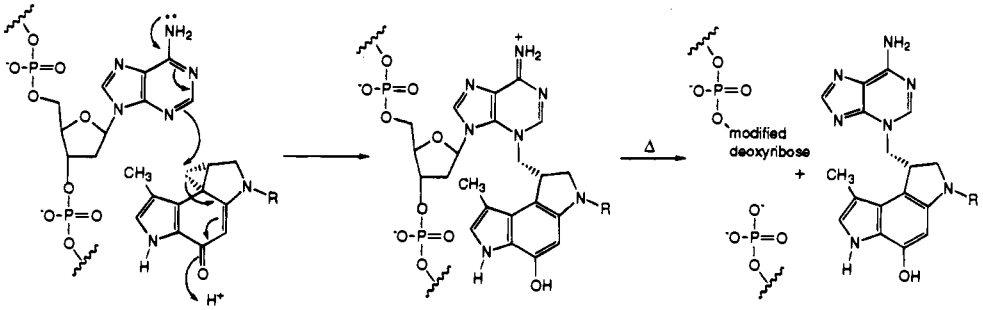

prevents the reverse reaction after alkylation has occurred[7,8] or keeps the drug bound so that it realkylates the same site.[9] Boger and co-workers have suggested that irreversibility of alkylation may be related to the delayed toxicity of some of these compounds.[7]

While N-3 of adenine is the primary target of this class of compounds, in some cases, alkylation of N-3 of guanine has been shown.[5,7,10,11] In general, this appears to account for only a small amount of the alkylation sites. However, guanine alkylation can be increased by the use of oligonucleotides which do not contain a high affinity site.[11] Interestingly, the addition of distamycin A (**1**) drastically increases guanine alkylation by duocarmycin A (**3**), a natural product related to **2**, at the expense of adenine alkylation.[10] These two compounds appear to cooperatively recognize 5′-(A·T)G(G·C)TG*G (G* is the site of alkylation), a sequence not alkylated by **3** alone.

Several studies have shown that the unnatural enantiomers of this class of compounds also alkylate DNA and possess cytotoxic activity, in some cases comparable to that of the natural enantiomer.[5-7] Both enantiomers primarily alkylate N-3 of adenine, but the orientation of the drug is different. For the natural (+) enantiomer, the B and C subunits lie on the 5′ side of the site of alkylation but, on the 3′ side, for the (−) enantiomer as shown by DNA footprinting.[5] They also show different sequence selectivities, although both prefer A·T rich sites. (+) and (−) Analogs which contain only the A subunit do not show different sequence selectivity demonstrating the importance of the B and C subunits in determining the site of alkylation.[5-7] The unnatural enantiomer appears to be less reactive and provide less stabilization of the DNA helix as judged by the change in melting temperature of the alkylated DNA. A slight increase in the amount of alkylation on guanine was observed for (−)-**2**.[5] Only the natural enantiomer appears to cause delayed death.[5]

Several groups have conducted NMR studies of the nature of the adducts formed by this class of compounds with oligonucleotides.[2,12-17] One early study showed that (+)-**2** did bind in the minor groove oriented in a 3′ to 5′ manner.[2] Powers and Gorenstein have determined the restrained molecular dynamics structure of an adduct formed by CPI-$CDPI_2$, an analog which lacks the oxygen substituents on the B and C units.[12] Hurley and co-workers have studied a different (+)-**2**−oligonucleotide adduct, especially the presence of ordered water molecules and the helix bending induced by complex formation but have not yet published full structural details.[13-16] Lin and Patel have published a preliminary report on a duocarmycin A−triplex adduct.[17]

Design Rationale and Experimental Strategy. Studies on **1** and related compounds have led to the concept of lexitropsins

(10) Yamamoto, K.; Sugiyama, H.; Kawanishi, S. *Biochemistry* **1993**, *32*, 1059−1066.
(11) Sugiyama, H.; Ohmori, K.; Chan, K. L.; Hosoda, M.; Asai, A.; Saito, H.; Saito, I. *Tetrahedron Lett.* **1993**, *34*, 2179−2182.
(12) Powers, R.; Gorenstein, D. G. *Biochemistry* **1990**, *29*, 9994−10008.
(13) Lin, C. H.; Hill, G. C.; Hurley, L. H. *Chem. Res. Toxicol.* **1992**, *5*, 167−182.
(14) Sun, D.; Lin, C. H.; Hurley, L. H. *Biochemistry* **1993**, *32*, 4487−4495.
(15) Lin, C. H.; Beale, J. M.; Hurley, L. H. *Biochemistry* **1991**, *30*, 3597−3602.
(16) Lin, C. H.; Hurley, L. H. *Biochemisty* **1990**, *29*, 9503−9507.
(17) Lin, C. H.; Patel, D. J. *J. Am. Chem. Soc.* **1992**, *114*, 10658−10660.

or information-reading peptides.[18] Rational structural modifications have been made to these natural products to change their sequence specificity and binding characteristics. For example, replacement of one of the pyrrole rings with an imidazole or other heterocycle which can accept a hydrogen bond from G-2-NH_2 allows G·C base pairs to be recognized. We decided to apply the lexitropsin concept to CC-1065 analogs. The B and C subunits of **2** have been shown to influence binding, sequence selectivity, and bioactivity (*vide supra*). In principle, they can be replaced by other moieties which confer these same properties.

We have synthesized a series of compounds which contain the CPI moiety coupled with various lexitropsins.[19] Two of the most potent CPI-lexitropsin hybrids synthesized so far, CPI-APB (**4**) and CPI-AP_2B (**5**), have the CPI unit linked to one or two *N*-methyl pyrroles via a *trans* double bond.[20] This spacer has previously been found to have nearly ideal characteristics for joining ligands.[21] The propyl end group has also been found to increase the bioactivity of these compounds which are extremely cytotoxic compounds (IC_{50} for KB cells of 0.76 and 0.95 fg/L, respectively). They were synthesized and tested in racemic form so the contributions of the individual enantiomers is currently unknown. DNA autocleavage assays[22] have shown that these two compounds bind to A·T rich regions of DNA and, upon heating, cause strand cleavage in a manner similar to that exhibited by **2**.[19] These assays revealed that **4** and **5** had a slightly different sequence preference from **2**. There was also detectable alkylation of guanine.

Detailed information on the location and orientation of the drug on the DNA, structure and stereochemistry of the covalent adducts is necessary in order to proceed with informed structure modification. Therefore in this paper, we report the three-dimensional structure determined by ^{1}H-NMR and restrained molecular dynamics of a complex of **4** bound to the decamer d(CGCAATTGCG)$_2$. Compound **4** was chosen for this study over **5** because it is smaller and would be expected to produce fewer ambiguous drug assignments. Since **4** was synthesized in the racemic form, either enantiomer could react with the oligonucleotide. It might be expected that the enantiomer corresponding to (−)-**2** would preferentially react since this would allow the molecule to alkylate one of the adenines with the rest of the drug oriented 3′ to that adenine in the A·T tract (*vide supra*).

Experimental Section

Synthesis. The synthesis and characterization of CPI-APB (**4**) has been reported separately.[19] The oligonucleotide d(CGCAATTGCG)$_2$ was prepared as described previously.[23] To form the complex, 2 μmol of the oligonucleotide was dissolved in 1 mL of water containing 10 mM sodium phosphate buffer and 100 mM NaCl, pH 7.0, and lyophilized. This sample was redissolved in 1.8 mL of water to which 2 mg (4.8 μmol) of racemic **4**, dissolved in 100 μL of DMF and 100 μL of acetone, was added. This yellow solution was allowed to stand at room temperature for 1 week. The solution was then applied to three C_{18} Sep-Pak cartridges (Waters) connected in series. These were washed with water to remove salts and then eluted with 10% CH_3CN in water to give the adduct mixed with small amounts of the free duplex. A UV absorbance spectrum of the product showed a new absorbance at 396 nm, in addition to the duplex absorbance at 258 nm.

NMR Spectroscopy. The products of several alkylation reactions were combined and dissolved in 0.5 mL of 99.9% D_2O containing 10 mM sodium phosphate buffer and 100 mM NaCl, pH 7.0 and lyophilized. The sample was again lyophilized from 99.9% D_2O and then from 99.96% D_2O and finally dissolved in 0.5 mL of 99.96% D_2O. All spectra were acquired on a Varian Unity 500 spectrometer at 25 °C, unless otherwise specified. The two-dimensional spectra were acquired on a nonspinning sample in a phase-sensitive manner using the States−Haberkorn method.[24] Data sets were multiplied by a 60° shifted sinebell function in both directions prior to Fourier transformation. Either the baseline correction method of Otting et al.[25] or a spline correction (where a baseline correction function, defined by connecting multiple straight line segments between baseline regions, is subtracted)[26] were used. In general, a sweep width of 4600 or 4300 Hz was used. Either 2K or 4K data points were collected in t_2 and 450−1024 FID's in t_1 with 64−120 transients for each. A relaxation delay of 1−2 s was used with a homospoil pulse prior to each transient.

The standard pulse sequences were used for DQFCOSY[27] and T_1 inversion-recovery experiments.[28] A series of NOESY[24] spectra were acquired with mixing times of 50, 80, and 250 ms. A ROESY[29] experiment was run with a 50 ms mixing time. The transmitter offset was moved downfield to 6.5 ppm, and the sweep width widened to 6000 Hz to reduce Hartmann−Hahn artifacts.[30] A 2-kHz spin-lock field was generated by a series of 30° pulses. A MINSY experiment was performed where the H2′/H2″ region centered at 2.27 ppm was irradiated during the mixing period of 250 ms.[30] A series of TOCSY spectra using an MLEV-17 sequence to generate the spin-lock field were acquired with mixing times of 30, 50, 70, and 120 ms.

The sample was also dissolved in 9:1 H_2O:D_2O to study the exchangeable protons. NOESY spectra (200 and 250 ms mixing times) were acquired using either presaturation,[33] the Sklenar−Bax method (soft $90°_{-y}-90°_{\phi}$−spin lock$_{\psi}$, $\phi = x, -x, x, -x$, $\psi = y, y, -y, -y$),[34] or NODE-1[35] shaped pulse water suppression techniques. In the latter two cases, these pulse sequences replaced the final 90° pulse of the normal NOESY pulse sequence. For the NOESY spectrum incorporating a NODE-1 pulse, data shifting and linear prediction were used to remove frequency-dependent phase shifts as described by Smallcombe.[26] Also the time domain convolution difference method of Marion et al. was used to further reduce the residual water signal during data processing.[36]

Model Building and Simulation Protocol. Initial noncovalent models of both enantiomers of **4** with d(CGCAATTGCG)$_2$ were generated by graphically docking the drug molecule into the minor groove of the DNA in Arnott B-DNA conformation using in-house graphics software. Initially the drugs were placed in suitable positions for covalent binding with the cyclopropyl ring opened and so possessed an unsatisfied valence at the alkylating carbon (C4). These docked geometries were now subjected to energy minimization without any NOE constraints, using an in-house implementation of the AMBER force field within the PROMETHEUS program suite. This program

(18) Lown, J. W. *Chemtracts: Org. Chem.* **1993**, 205−237.
(19) Wang, Y.; Luo, W.; Lown, J. W. *Anti-Cancer Drug Design* in press.
(20) These names are used to indicate the structues: A = acrylate, P = *N*-methylpyrrole, and B = butyramide.
(21) Rao, K. E.; Zimmermann, J.; Lown, J. W. *J. Org. Chem.* **1991**, *52*, 786−797.
(22) Gupta, R.; Xie, G.; Lown, J. W. *Gene* **1994**, *149*, 81-90.
(23) Lee, M.; Chang, D.-K.; Harley, J. A.; Pon, R. T.; Krowicki, D.; Lown, J. W. *Biochemistry* **1988**, *27*, 445−455.
(24) States, D. J.; Haberkorn, R. A.; Ruben, D. J. *J. Magn. Reson.* **1982**, *48*, 286−292.
(25) Otting, G.; Widmer, H.; Wagner, G.; Wüthrich, K. *J. Magn. Reson.* **1986**, *66*, 187−193.
(26) Smallcombe, S. J. *J. Am. Chem. Soc.* **1993**, *115*, 4776-4785.
(27) Vold, R. L.; Waugh, J. S.; Klein, M. P.; Phelps, D. E. *J. Chem. Phys.* **1968**, *48*, 3831-3832.
(28) Rance, M.; Sorenson, O. W.; Bodenhausen, G.; Wagner, G.; Ernst, R. R.; Wütherich, K. *Biochem. Biophys. Res. Commun.* **1983**, *117*, 479-485.
(29) Bothner-By, A. A.; Stephens, R. L.; Lee, J-M.; Warren, C. D.; Jeanloz, R. W. *J. Am. Chem. Soc.* **1984** *106*, 811-813.
(30) Bax, A.; Davis, D. G. *J. Magn. Reson.* **1985**, *63*, 207-213.
(31) Massefski, W., Jr.; Redfield, A. G. *J. Magn. Reson.* **1988**, *78*, 150−155.
(32) Bax, A.; Davis, D. G. *J. Magn. Reson.* **1985**, *63*, 355-360.
(33) Rajagopal, P.; Gilbert, D. E.; van der Marel, G. A.; van Boom, J. H.; Feigon, J. *J. Magn., Reson.* **1988**, *78*, 526−537.
(34) Sklenar, V.; Bax, A. *J. Magn. Reson.* **1987**, *75*, 378−383.
(35) Liu, H.; Weiss, K.; James, T. L. *J. Magn. Reson. A* **1993**, *105*, 184−192.
(36) Marion, D.; Ikura, M.; Bax, A. *J. Magn. Reson.* **1989**, *84*, 425−430.

and force field was used for all subsequent minimizations and molecular dynamics. Minimization under *in vacuo* conditions with a distance dependent dielectric was achieved using an initial 20 steepest descent steps, followed by as many conjugate gradient steps as were necessary to achieve a gradient of ≤0.09 kcal/Å without any nonbonded cut-off limit.

The distance between alkylating carbon **4** of N3 of ^{4}A was maintained using a distance constraint of 100 kcal/mol/Å^2 and an equilibrium distance of 1.5 Å. The resultant minimized structures were then taken, and the appropriate covalent bond was formed. These covalent adducts were energy minimized using the same conditions as given previously without any NOE constraints.

Imposition of NOE constraints was achieved via a half-harmonic constraining function as follows:

$$E_{NOE} = K_{NOE}(R_{NOE} - R_{actual})^2 \quad \text{for } R > R_{NOE} \qquad (1)$$

$$E_{NOE} = 0 \quad \text{for } R < R_{NOE} \qquad (2)$$

The use of the above two equations means that nonbonded vdW and coulombic interactions were effectively the lower bound for the distance constraints. A total of 303 NOESY-derived distance constraints were then added for each adduct, with distance constraints of 15 kcal/Å^2 and an upper-bound of 5.0 Å for weak NOEs, 50 kcal/Å^2 and an upper-bound of 3.3 Å for medium NOEs, and 150 kcal/Å^2 and an upper-bound of 2.7 Å for strong NOEs. The global NOE constraint was equal to 19 450 kcal/mol/Å^2. Restrained energy minimization now followed with the same minimization conditions as previously performed, *i.e.*, distance dependent dielectric and no nonbonded cut-off limit. Constant temperature *in vacuo* restrained molecular dynamics was now performed at 300 K for 100 ps with equilibration to 300 K over the first 5 ps. All bonds were constrained during the course of the simulation using the RATTLE[33] algorithm and the step-size employed was 0.001 ps. No Watson–Crick constraints were employed in any part of the simulation. Energetic analysis of the molecular dynamics run was performed every 0.1 ps.

Parameterization. Novel bonded parameters were taken from MOPAC93[34] AMI[35] optimized geometries and employed appropriate existing AMBER[36,37] force constants. Point charges for ring-opened **4** and alkylated adenine were determined by fitting to molecular electrostatic potentials determined using the AM1 Hamiltonian at the AM1 optimized geometries within MOPAC93 (KEYWORD = ESP). Bonded parameters and point charges employed for novel fragments are given in Tables 1–5, with the keys to atom numbering and atom types given in Figures 1 and 2. Phosphate groups were completely neutralized in order to prevent the large repulsion which would occur between two unit negative moieties during *in vacuo* dynamics. This neutralization was performed by scaling the phosphate oxygen charges according to the ratio of the original oxygen charges, *i.e.*, phosphoryl oxygens were scaled to a larger extent than the diester oxygens. This resulted in a point charge on phosphodiester oxygens of −0.321 and a point charge on phosphoryl oxygens of −0.535. The alkylated adenine (^{4}A) was represented without neutralization, *i.e.*, a net charge of +1. In all other respects the parameters employed were identical to the original AMBER set.

Results and Discussion

Preparation and Characterization of Covalent Adduct. The alkylation of d(CGCAATTGCG)$_2$ by **4** proceeds readily at room temperature. A mixture of DMF and acetone was found necessary to solubilize **4** during the reaction while maintaining a low enough organic content (10%) to keep the oligonucleotide as a duplex. Upon complexation, the drug chromophore exhibits a bathochromic shift from 365 to 396 nm. This complex was stable over the several month period used to acquire the NMR data.

Although racemic **4** was used only one diastereomeric adduct was isolated as the major product. This suggests that highly

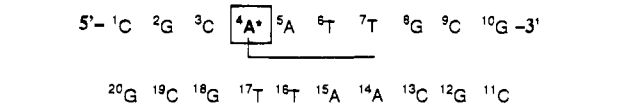

Figure 2. Depiction of the duplex decamer used in complex formation, site of covalent binding of **4**, and its orientation within the groove in the (*S*)-**4a** adduct.

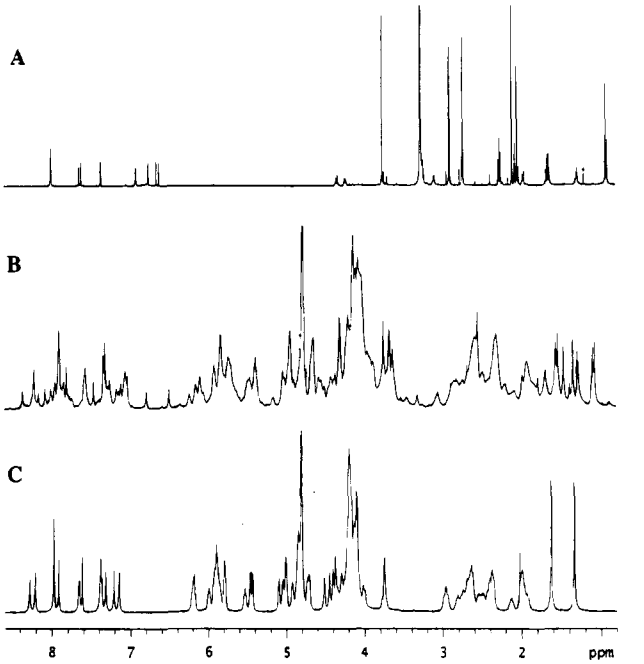

Figure 3. ^{1}H-NMR spectra of (a) CPI-lexitropsin **4** in DMF-d_7/acetone-d_6, (b) covalent complex in D_2O, and (c) free duplex decamer in D_2O.

preferential reactivity toward this oligonucleotide sequence is shown by one enantiomer of **4**. As discussed above, the oligonucleotide used should complex best with the enantiomer of **4** corresponding to (−)-CC-1065. Confirmation of the stereochemical purity of the diastereomer with the carbon at the point of attachment (4a) in the (*S*) configuration followed from the ^{1}H-NMR and restrained molecular modeling.

NMR Assignments for the Duplex d(CGCAATTGCG)$_2$ within the Covalent Complex. The ^{1}H NMR assignments for the free decamer (Figure 2) have been previously reported.[23] Upon alkylation with **4**, the symmetry of the decamer is lost as shown by the doubling of essentially all of the proton signals (Figure 3). As discussed below, one major adduct was observed, although a trace of the decamer that was not alkylated remained as evidenced by the characteristic thymidine methyl signals (1.30 and 1.60 ppm) of the free duplex.

The nonexchangeable oligonucleotide protons of the complex were assigned on the basis of sequential NOE correlations observed between the aromatic base protons (H8/H6) and the sugar protons as expected of a right-handed helix.[37,38] The NOESY spectrum with the 250 ms mixing time was primarily used to make the assignments. The spin diffusion from the long mixing time allowed the base protons to show all the expected inter- and intraresidue NOEs to H1′, H2′, H2″, and H3′ as well as correlations between adjacent base protons. By tracing correlations from one base proton to the H1′ proton on the same residue and that on the preceding (5′) residue, the entire duplex could be assigned (Figure 4, Table 1). All H8/H6 assignments were cross checked by examining the NOEs to other H8/H6, H2′, H2″, and H3′ protons. Scalar correlations from DQFCOSY

(37) Feigon, J.; Sklenar, V.; Wang, E.; Gilbert, D. E.; Macaya, R. F.; Schultze, P. *Methods Enzymol.* **1992**, *211*, 235–253.

(38) Clore, G. M.; Gronenborn, A. M. *Crit. Rev. Biochem.* **1989**, *24*, 479–564, and references cited therein.

Table 1. ^{1}H Chemical Shifts[a] (ppm) of the Decamer Portion of the d(CGCAATTGCG)$_{2n}$–CPI-Lexitropsin Complex

base	H8	H6	H5	CH_3	H2	H1′	H2′	H2″	H3′	H4′	H5′/H5″	imino	CN4H$_a$[b]	CN4H$_b$[c]
^{1}C		7.61	5.86			5.73	1.95	2.37	4.69	4.05	3.71/3.67			
^{2}G	7.93					5.95	2.60	2.70	4.98	4.35	4.11/4.01	12.80		
^{3}C		7.82	5.87			5.19	2.30	2.53	4.92	4.33	4.17/4.12			
^{4}A	8.39				7.91	6.19	2.79	2.88	5.07	4.42	4.14/4.05			
^{5}A	7.97				8.10	5.95	2.34	2.67	4.53					
^{6}T		6.82		1.09		5.53	1.60	2.24	4.61	3.35	4.01/3.80	13.47		
^{7}T		7.08		1.49		5.75	1.96	2.36	4.83	3.90	3.49/	13.56		
^{8}G	7.86					5.78	2.62	2.66	4.97	4.34	4.08/3.97	12.66		
^{9}C		7.35	5.41			5.79	1.89	2.33	4.80	4.18	4.07/		8.41	6.53
^{10}G	7.93					6.13	2.61	2.36	4.67	4.17	4.07/	d		
^{11}C		7.61	5.86			5.73	1.95	2.37	4.69	4.05	3.71/3.67			
^{12}G	7.92					5.88	2.64	2.72	4.97	4.34	4.08/3.97	13.03		
^{13}C		7.29	5.43			5.49	1.83	2.23	4.80	4.10			8.40	6.34
^{14}A	8.24				7.37	5.77	2.77	2.84	5.05	4.39	4.12/4.01			
^{15}A	8.24				7.84	6.27	2.65	2.87	5.01	4.46	4.23/4.13			
^{16}T		7.14		1.37		5.95	1.93	2.45	4.80	4.23	4.10/	14.05		
^{17}T		7.09		1.56		5.52	1.74	1.85	4.60	4.07		14.03		
^{18}G	8.03					5.46	2.84	2.40	4.86	4.24	4.13/	d		
^{19}C		7.20	5.70			5.42	1.61	2.11	4.57	4.29			8.06	6.88
^{20}G	7.90					6.10	2.66	2.33	4.71	4.23	4.14/3.94	d		

[a] Proton chemical shifts referenced to HDO at 4.80 ppm. [b] CNH4$_a$ = hydrogen-bonded cytosine amino proton. [c] CNH4$_b$ = non-hydrogen-bonded cytosine amino proton. [d] Not assigned (see text).

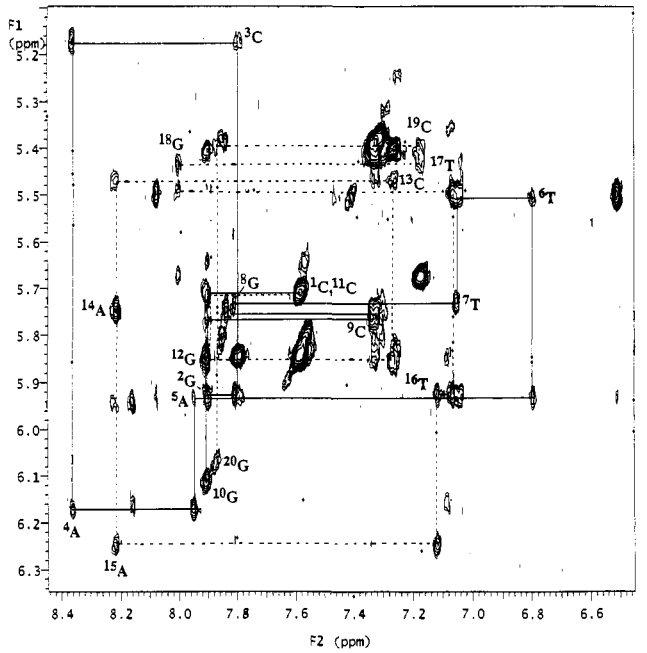

Figure 4. Expansion of the 2D-NOESY (250 ms) spectrum of the covalent complex showing the correlations between the aromatic protons and H1′/H5. The sequential connectivity of the base H8/H6 to H1′ is shown for strand 1 (alkylated, solid line) and strand 2 (broken line).

and TOCSY spectra allowed unambiguous assignments of TCH$_3$ and CH5 protons as well as confirming the individual sugar spin systems.

The sequential assignment method used requires that the oligonucleotide adopt a right-handed helix conformation, but it does not distinguish between A- and B-DNA forms. The most diagnostic difference between these two conformers is the distance between the H8/H6 base proton and the H3′ proton on the attached sugar. This distance is considerably shorter in A-DNA because of the change in sugar conformation from 2′-endo (B-DNA) to 3′-endo. However, observation of an NOE between these two protons does not necessarily imply an A-DNA type of structure because the correlation may result from spin diffusion through the H2′ and H2″ protons. This problem can be overcome by the MINSY (*m*ixing *i*rradiation during a *N*OESY) experiment.[31] In this experiment, the H2′/H2″ region is irradiated during the mixing period of a NOESY experiment to saturate these protons and prevent two-step magnetization transfer. In the MINSY spectrum, almost all of the H8/H6 to H3′ correlations were missing thus suggesting a B-type conformation. The only exceptions were the terminal residues of the two strands (^{1}C, ^{10}G, ^{11}C). The ROESY spectrum, which should also show significantly lower spin diffusion, confirms these results.[39,40] The AH2 signals were assigned along with those of the exchangeable protons from experiments conducted in 9:1 H_2O:D_2O (Figure 5).

Several different methods of suppressing the large water signal were used in conjunction with NOESY. No single spectrum contained all of the correlations needed to assign the imino and AH2 protons. However a combination of different methods allowed most to be determined as described below. It was noted that while simple presaturation gave the spectrum with the best signal-to-noise ratio, several of the exchangeable protons were suppressed, especially in the 13.0–13.3 ppm region (see supporting information). Immediately evident in the imino region of the ^{1}H spectrum is the presence of two protons which are shifted significantly downfield from any in the free oligonucleotide (14.05 and 14.03 ppm). The imino proton at 14.05 ppm shows a correlation to another imino at 13.47 ppm. The former also exhibits a strong NOE to 8.10 ppm and a somewhat weaker NOE to 7.84 ppm. The imino at 13.47 ppm shows correlations to both of these AH2 signals, although with reversed intensities as well as to 7.37 and 13.56 ppm. These last two protons also exhibit a strong NOE to each other. The H2 protons of adenine are known to sometimes show NOEs to the H1′ on the sugar to the 3′ side on the same strand and to the 5′ side on the opposite strand depending on the extent of propeller twisting.[37,38] The AH2 signal at 8.10 ppm exhibits an NOE to ^{17}H1′ at 5.52 ppm (possibly overlapping with an NOE to ^{6}TH1′ at 5.53 ppm), allowing its assignment as ^{5}AH2. Similar correlations establish ^{15}AH2 as the 7.84 ppm signal. This proton additionally shows a strong NOE to 7.37 ppm which must therefore be ^{14}AH2. Correlations from both 7.37 and 13.56 to 12.66 ppm indicate that the latter must be ^{8}GNH1 which is further correlated to ^{12}CNH1 (13.03 ppm).

(39) Bothner-By, A. A.; Stephens, R. L.; Lee, J.-M.; Warren, C. D.; Jeanloz, R. W. *J. Am. Chem. Soc.* **1984**, *106*, 811–813.
(40) Bauer, C. J.; Frenkiel, R. A.; Lane, A. N. *J. Magn. Reson.* **1990**, *87*, 144–152.

Surprisingly, the remaining AH2 proton showed no correlations to any imino protons, suggesting some sort of disrupton of the helix structure. As will be discussed below, ^{4}AH2 is assigned as 7.91 ppm on the basis of several NOEs to drug protons. It should be noted that this proton is on the base which is alkylated. A weak NOE from ^{5}AH2 to the other downfield imino signal (14.03 ppm) indicates that this proton can be assigned as ^{17}TNH3. Because of the small chemical shift difference between this proton and ^{16}TNH3 (14.05 ppm), no NOE could be observed between them. Correlations from GNH1 and CH5 protons established the identity of some of the guanine amino protons, and, in particular, demonstrated that signal at 12.80 ppm is ^{2}GNH1. Due to a lack of correlations under several different experimental conditions, the remaining imino protons could not be unambiguously assigned. These protons appear in the 13.0−13.3 ppm region, and all exchange very rapidly with bulk water as evidenced by their reduction or elimination by presaturation of the water signal and by exchange crosspeaks with the water signal in NOESY experiments in which the read pulse does not excite the water.[26]

NMR Assignments for the Drug within the Covalent Complex. Scalar correlations observed in the DQFCOSY and TOCSY spectra provided a good starting point for making drug assignments (Table 2). Two correlations are observed in the aromatic to aromatic region (7.77/7.08 and 7.49/6.53 ppm). The latter is much weaker, and these two protons appear as singlets in the 1D spectrum so this pair can be assigned to the pyrrole unit. The much more strongly coupled pair (7.77 and 7.08 ppm) must therefore be due to the trans double bond.

A weak correlation between 7.35 and 2.58 ppm combined with the observation that the latter is a large sharp singlet allows the assignment of these two signals as H-2 and 3-CH_3, respectively. Crosspeaks linking 1.71 ppm to both 2.52 and 1.13 ppm must result from the propyl chain. Strong NOESY correlations between both 7.77 and 7.49 ppm to the singlet at 3.79 ppm suggest that these protons can be assigned as H-3′, H-7′, and 8′-NCH_3, respectively. Another strong NOE was observed between 7.08 and 6.53 ppm, confirming their assignments as H-2′ and H-5′, respectively.

The remaining protons on the former CPI unit were assigned as follows. Two pairs of protons (3.09/2.90 and 3.65/3.11 ppm) exhibit strong NOE and scalar correlations, indicating that these are the geminal protons on C4 and C5. NOEs from 3-CH_3 to both 3.09 and 2.90 suggest that these protons are H-4A and H-4B. The other geminal pair (3.65/3.11 ppm) both show weak TOCSY correlations and moderate NOEs to 2.01 ppm which must be H-4a. The TOCSY correlations to 2.01 ppm are most likely weak due to small coupling constants and partial cancellation by ROESY artifacts which have the opposite sign. No scalar correlations were observed between H-4a and 3.09 or 2.90 ppm. The coupling constant between 2.01 and 2.90 ppm is probably close to zero, as is observed for the CC-1065−adenine adduct,[2] while the correlation between 2.01 and 3.09 ppm may be obscured by the stronger one between 2.01 and 3.11 ppm. The chemical shifts for H-4A and H-4B have moved significantly downfield, indicating the opening of the cyclopropyl ring.

No correlations were observed to H-7 so this proton was not assigned. This proton is on the convex face of the drug and thus, as discussed below, should point away from the oligonucleotide. The location of the two NH proton signals could be determined from NOESY spectra acquired in 9:1 H_2O:D_2O (Figure 5). The signal at 10.31 ppm exhibited a strong NOE to H-2, while the signal at 8.83 ppm showed NOEs to 11′-CH_2 and H-5′. Thus these exchangeable protons must be 1-NH and

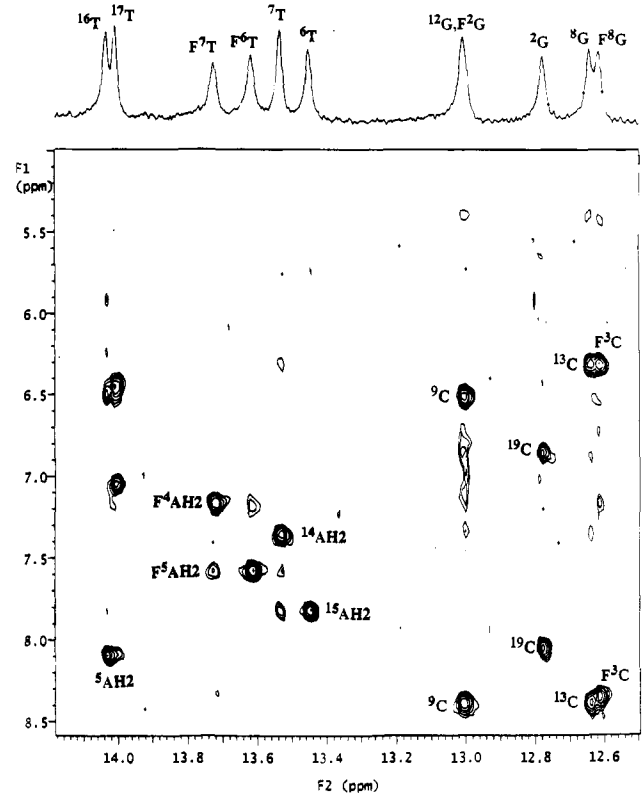

Figure 5. Expansion of the NOESY spectrum (250 ms) of the covalent complex in 9:1 H_2O:D_2O at 25 °C, using presaturation of the water signal, showing the correlations between the imino protons and the AH2 and cytosine amino protons. Note that some imino protons are suppressed by the presaturation. Signals marked by F arise from the free duplex.

9′-NH, respectively. A doublet can be observed in the 1D spectrum for the signal at 7.77 ppm, but the proton at 7.08 ppm appears in too crowded a region to determine its multiplicity. Figures 4 and 5 summarize the important NOEs used to assign the drug protons.

Structure of the Complex: Regiochemistry and Stereochemistry of Drug Binding. A number of NOEs were observed between the drug and the oligonucleotide which allowed the general placement of the drug in the minor groove (Table 2, Figure 4). Both 3-CH_3 and H-4B show strong NOEs to ^{4}AH1′, implying that ^{4}A is the site of alkylation. Three protons from the former CPI unit (H-4a, H-5A, and H-5B) all correlate to a signal at 7.91 ppm in the NOESY spectrum. This signal was not previously assigned and shows no correlations to any oligonucleotide protons. If ^{4}A is the site of alkylation, these three protons should be close to ^{4}AH2 which could not be assigned by normal methods (see above). T_1 measurements indicate that the proton at 7.91 ppm relaxes more slowly than most of the oligonucleotide protons, as expected for an AH2.

NOEs are observed to all of the other AH2 protons. H-2′, H-5′, and 9′-NH all are correlated to ^{5}AH2. This amide proton, along with those of the propyl chain, appear close to ^{15}AH2, while the propyl methyl group also exhibits an NOE to ^{14}AH2. The NOEs between 9′-NH and both ^{5}AH2 and ^{15}AH2 suggest possible hydrogen bonds between this amide proton and the minor groove thymidine oxygens on the base pairs to these adenines (^{16}TO2 and ^{6}TO2, respectively). In addition, the propyl protons all have crosspeaks to ^{7}TH1′. NOEs were also observed between +^{17}TH1′ and H-4a, H-2′, and H-5′. These correlations and other listed in Table 1 and shown in Figure 6b clearly indicate that the drug lies in the minor groove and extends in a 5′ to 3′ direction. This indicates that the enantiomer analogous

Table 2. ^{1}H Chemical Shifts and NOESY Crosspeaks of the Ligand Portion of the d(CGCAATTGCG)$_2$–CPI-Lexitropsin Complex

H no.	4[a]	complex	Δδ[b]	ligand–ligand NOEs[c]	ligand–DNA NOEs[c]
1-NH	10.49	10.31	-0.18	H-2 (s)	
H-2	6.88	7.35	+0.47	1-NH (s), 3-CH$_3$ (s), H-4B (w)	^{3}CH5 (m)
3-CH$_3$	2.03	2.58	+0.55	H-2 (s), H-4A (w), H-4B (s)	^{4}AH1′ (s), ^{4}AH3′ (w), ^{19}CH1′ (m), ^{2}GNH1 (w)
H-4A	1.94[d]	3.09	+1.15	3-CH$_3$ (w), H-4B (s)	^{5}AH3′ (m), ^{17}TNH3 (w)
H-4B	1.27[d]	2.90	+1.63	H-2 (w); 3-CH$_3$ (s), H-4A (s)	^{4}AH1′ (s), ^{5}AH3′ (w)
H-4a	3.05	2.01	+1.04	H-5A (m), H-5B (m)	^{4}AH2 (w), ^{17}TH1′ (m), ^{19}CH1′ (w)
H-5A	4.18[d]	3.11	−1.07	H-4a (m), H-5B (s)	^{4}AH2 (w)
H-5B	4.29[d]	3.65	−0.64	H-4a (m), H-5A (s)	^{4}AH2 (w)
H-7	6.73[e]				
H-2′	6.59	7.08	+0.49	H-5′ (s)	^{5}AH2 (m), ^{17}TH1′ (m)
H-3′	7.60	7.77	+0.17	8′-NCH$_3$ (s)	^{6}TH4′ (m)
H-5′	6.67	6.53	−0.14	H-2′ (s), 9′-NH (m)	^{5}AH2 (s), ^{6}TH4′ (w), ^{15}AH2 (w), ^{17}TH1′ (s)
H-7′	7.33	7.49	+0.16	8′-NCH$_3$ (s)	^{7}TH4′ (s), ^{7}TH5′ (m), ^{17}TH1′ (w)
8′-NCH$_3$	3.75	3.79	+0.04	H-3′ (s), H-7′ (s)	^{5}AH2 (w), ^{6}TH1′ (w), ^{6}TH3′ (w), ^{6}TH4′ (m), ^{7}TH4′ (w), ^{7}TH5′ (w)
9′-NH	8.99	8.83	−0.16	H-5′ (m), 11′-CH$_2$ (s)	^{5}AH2 (w), ^{15}AH2 (m)
11′-CH$_2$	2.24	2.52	+.028	9′-NH (s), 12′-CH$_2$ (m), 13′-CH$_3$ (w)	^{6}TNH3 (w), ^{7}TH1′ (w), ^{15}AH2 (s)
12′-CH$_2$	1.64	1.71	+0.07	11′-CH$_2$ (m), 13′-CH$_3$ (s)	^{7}TH1′ (w), ^{15}AH2 (m)
13′-CH$_3$	0.92	1.13	+0.21	11′-CH$_2$ (w), 12′-CH$_2$ (s)	^{7}TH1′ (m), ^{14}AH2 (m), ^{15}AH2 (m), ^{15}AH1′ (w)

[a] In DMF-d_7/acetone-d_6. [b] Δδ = δ(complex) − δ(**4**). [c] s = strong, m = moderate, w = weak intensity. [d] The assignments for H-4A/H-4B and H-5A/H-5B may be reversed. [e] Very broad signal.

Table 3. Chemical Shift Changes (Δδ) between the Complex and the Free Duplex[a]

base	H8	H6	H5	CH$_3$	H2	H1′	H2′	H2″	H3′	H4′	H5′/H5″	imino	CN4H$_a$[b]	CN4H$_b$[c]
^{1}C		−0.02	−0.06			−0.04	−0.01	−0.03	−0.01	−0.02	0/			
^{2}G	−0.01					0.06	0	−0.02	−0.01	0	0.02/0.03	−0.24		
^{3}C		0.46	0.43			−0.32	0.33	0.18	0.09	0.17	0.11/			
^{4}A	0.14				0.73	0.21	0.01	−0.06	0	0	0/0			
^{5}A	−0.21				0.51	−0.23	−0.26	−0.26	−0.49					
^{6}T		−0.30		−0.21		−0.35	−0.36	−0.29	−0.19	−0.83	−0.15/	−0.17		
^{7}T		−0.21		−0.11		−0.11	−0.14	−0.10	−0.06	−0.25	−0.59/	−0.19		
^{8}G	−0.03					−0.06	0	0	−0.02	−0.04	−0.05/−0.13	0.02		
^{9}C		0	−0.01			0.01	−0.01	−0.01	−0.01	0.01			−0.03	0
^{10}G	−0.02					−0.03	−0.01	−0.01	0	0	0/	d		
^{11}C		−0.02	−0.06			−0.04	−0.01	−0.03	−0.01	−0.02	0/			
^{12}G	−0.02					−0.01	0.04	0	0	−0.01	−0.01/−0.01	−0.01		
^{13}C		−0.07	−0.01			−0.02	−0.14	−0.12	−0.03	−0.06			0.03	−0.01
^{14}A	−0.01				0.19	−0.21	−0.01	−0.10	−0.02	−0.03	−0.03/−0.05			
^{15}A	0.06				0.25	0.09	0.05	−0.06	−0.01	−0.02	−0.03/−0.02			
^{16}T		−0.02		0.07		0.07	−0.03	−0.08	0	0.05	−0.06/	0.41		
^{17}T		−0.20		−0.04		−0.34	−0.36	−0.61	−0.29	−0.08		0.28		
^{18}G	0.14					−0.38	0.22	−0.26	−0.13	−0.14	0/	d		
^{19}C		−0.15	0.28			0.36	−0.29	−0.23	−0.24	0.12			−0.38	0.35
^{20}G	−0.05					−0.06	0.04	−0.04	0.04	0.06	0.07/			

[a] Δδ = δ(complex) − δ(free) underlined are ≤0.3 ppm. [b] CNH4$_a$ = hydrogen-bonded cytosine amino proton. [c] CNH4$_b$ = non-hydrogen-bonded cytosine amino proton. [d] Not assigned (see text).

to (−)-CC-1065 was the one that reacted with the decamer.[5-7] Almost all of the NOEs observed between the drug and the decamer are to protons on the concave face of the drug. This orientation and regiochemistry of the drug within the groove requires an (*S*) configuration of the newly created stereocenter from the original cyclopropane ring. This conclusion is in accord with the results of the restrained molecular dynamics calculations (see below).

Changes in the chemical shifts between the free drug and decamer and the complex also indicate the positioning of the drug in the minor groove (Tables 2 and 3). The largest perturbations are observed in the central region of the decamer, especially the second through the sixth base pairs. Most of the large chemical shift differences are upfield shifts, suggesting that these protons could be in the shielding cones of the aromatic rings of the drug. Some of the most significant chemical shift changes are observed for the H2 protons of adenine. Notably, this difference is largest for ^{4}AH2 (Δδ +0.73 ppm), which is on the base which is alkylated, and decreases for each base further to the 3′ side. The effects are not limited to minor groove protons (H2, H1′, etc.); similarly large effects are exhibited by H2′ and H2″ and other major groove protons. This indicates that binding of the drug induces structural changes throughout the central region of the duplex.

From an examination of the energy minimized structures (Figures 7 and 8) it appears that the alkylation of ^{4}A causes propeller twisting of this base out of coplanarity with its base pair (^{17}T), thus disrupting the normal patterns of NOEs for imino and AH2 protons. The structures also suggest that the 9′-NH could be hydrogen-bonded to ^{16}TO2 and ^{6}TO3 and that ^{6}T is also propeller twisted, possibly due to such a hydrogen bond. This conclusion is consistent with the chemical shift changes in this region. The significant changes in chemical shift associated with the 3C/18G base pair may be due to either conformational changes or ring-current effects of the pyrrolindole unit. Ring current effects may also be responsible for the large Δδ observed for ^{6}TH1′, ^{6}TH4′, and ^{17}TH2″.

Molecular Modeling and Molecular Dynamics. During the course of the molecular dynamics simulation, the distance constraint contributions were very similar for both diastereomeric adducts. However, the total energy was consistently lower for one diastereomeric adduct by ~40 kcal/mol (Table 4). The origin of this total energetic difference is solely in the potential energy with kinetic energy being essentially identical for both

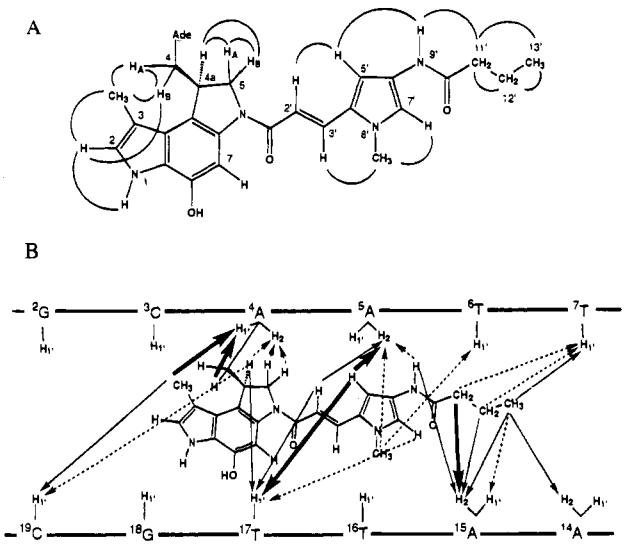

Figure 6. (a) Depiction of the intraligand NOE interactions used to assign the ligand protons. (b) Some of the ligand-DNA NOE interactions used in the deduction of structural features of the covalent complex. Bold arrows = strong NOEs, solid arrows = moderate NOEs, dashed arrows = weak NOEs.

Table 4. Averaged Energy Components of the Diastereomeric Complexes from 95 ps of Molecular Dynamics at 300 K

	adduct derived from	
energy component (kcal/mol)	(*R*)-**4**	(*S*)-**4**
av total energy	42.07 ± 14.36	−0.42 ± 10.34
av potential energy	−351.74 ± 13.80	−395.14 ± 11.26
av kinetic energy	393.81 ± 13.01	394.72 ± 11.23
av NOE constraint energy	21.06 ± 3.64	20.89 ± 3.69

adducts (as one would expect for constant temperature dynamics). Mean results of the analysis of component energies for 95 ps of productive restrained dynamics are given in Table 4 with standard deviations given as pseudo-errorbars (1 data point every 0.1 ps = 950 data points). The diastereomeric adduct which was consistently lower in energy was taken to represent the actual adduct studied by ^{1}H-NMR. The more favorable diastereomeric adduct was determined as that with the chiral carbon in the (*S*) configuration in accord with the ^{1}H-NMR analysis of the complex. A representative molecular dynamics structure of this more favorable diastereomeric adduct is given in Figures 7a and 8. A representative structure of the less

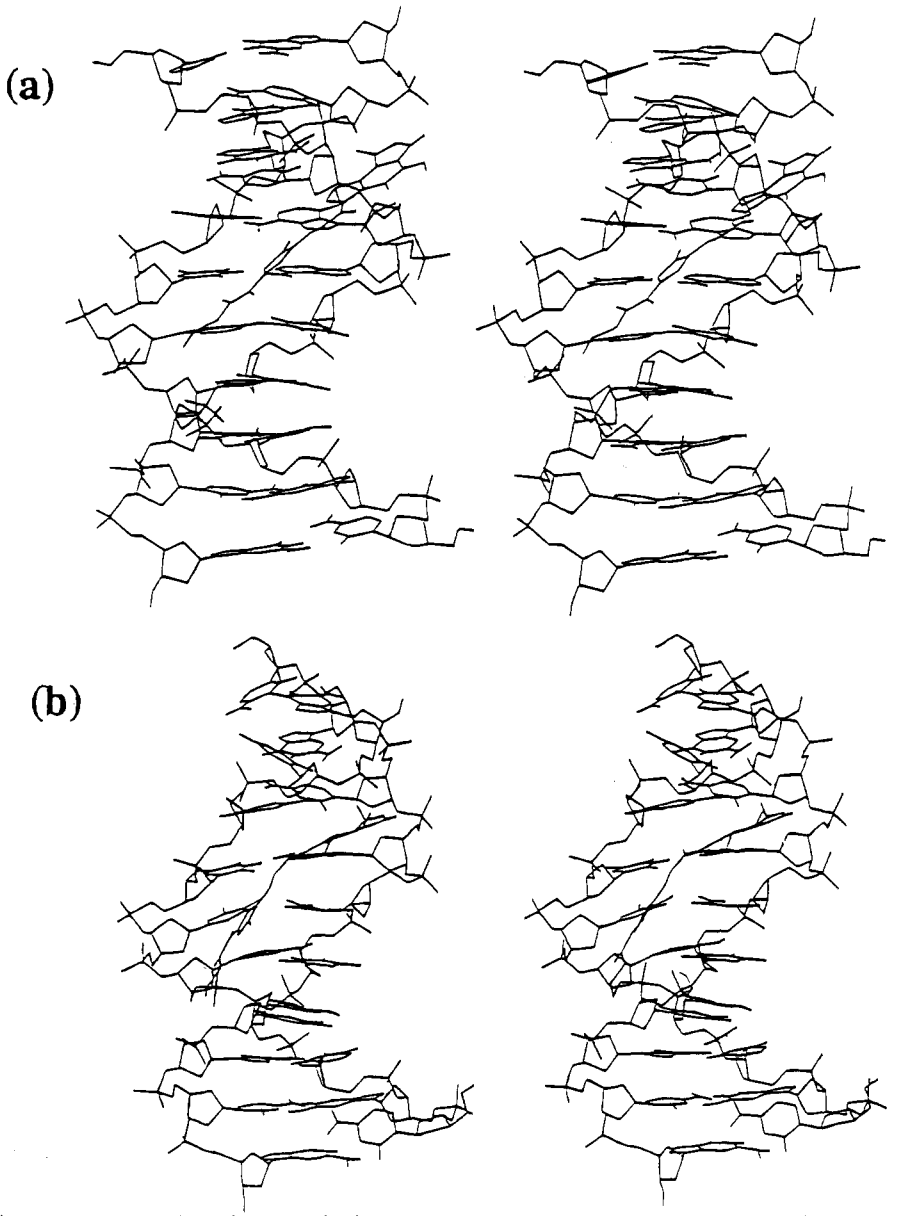

Figure 7. (a) Stereo pair of the preferred **4**-d(CGCAATTGCG)$_2$ adduct **4a** (*S*) diastereomer and (b) stereo pair of the corresponding less stable **4a**-(*R*)-diastereomer adduct.

Figure 8. Depiction of structure of the preferred **4a**-(*S*) diastereomeric adduct showing location of drug in space filling form.

favorable DNA adduct with the *R*-enantiomer is given in Figure 7b. In order for the *R*-enantiomer to bind, it must bend itself and significantly distort the duplex helix, while the *S*-enantiomer remains essentially planar and causes less disruption of the helix on binding. In the *S*-enantiomer, ^{4}A is twisted out of planarity with its base pair, explaining the lack of NOEs from ^{4}AH2 to other oligonucleotide protons. A determination was made of the deviation between target distances and distances achieved from the restrained simulation. The average value in Å for all (20) dynamics snapshots with their standard deviations are in Table 5.

The values in Table 5 are similar for both chiral forms, with the *S*-enantiomer giving very slightly better fitting to the target distances.

Table 5

	average deviation (Å)		rms deviation (Å)	
ligand chirality	r1 + r2/2 target	closest of r1/r2	r1 + r2/2 target	closest of r1/r2
(*R*-)	0.471 ± 0.008	0.301 ± 0.006	0.630 ± 0.014	0.398 ± 0.008
(*S*-)	0.461 ± 0.008	0.298 ± 0.007	0.619 ± 0.001	0.393 ± 0.0100

Conclusions

The racemic CPI-lexitropsin conjugate **4** reacted readily with the duplex oligonucleotide d(CGCAATTGCG)$_2$ to form a single covalent adduct as the major product. The product exhibits a new absorption band at 396 nm characteristic of the bound ligand that assists in the isolation and purification of the complex. ^{1}H-NMR analysis confirms *via* chemical shift changes and NOEs between protons in the drug and in the duplex that covalent attachment has taken place at ^{4}A. Moreover the drug is aligned in the 5′ to 3′ direction at the AATT core resulting from the selective binding of one enantiomer of **4** corresponding to that of (−)-CC-1065. The stereochemistry at the site of attachment at the 4a position of the drug is *S*, an inference that is corroborated by the restrained molecular dynamics simulation. In effect, the chiral DNA template has resolved the racemic **4** by selectively reacting with one of the enantiomers. The covalent adduct appears to be quite stable and showed no sign of reversibility such as has been observed with other CPI-derived agents.[7−9] It remains to be seen if this unusual stability and snug fit of all parts of **4** within the minor groove accounts for the exceptional cytotoxic potency (IC_{50}) of 0.76 fg/L.

Acknowledgment. This research was supported by a contract (with J.W.L.) from Taiho Pharmaceuticals Co. Inc., Hanno, Japan and by the Department of Chemistry, University of Alberta. Synthesis of DNA was carried out in the laboratories in Calgary (R.T.P.).

Supporting Information Available: Figure showing atom numbering used in the molecular mechanics computations on **4** and a table of atom types and point charges for **4** and the corresponding covalent adducts and five figures showing the 1D and 2D NOESY and TOCSY spectra of the d(CGCAATTGCG)$_2$/CPI-lexitropsin complex in D_2O and 9:1 H_2O:D_2O (8 pages). This material is contained in many libraries on microfiche, immediately follows this article in the microfilm version of the journal, can be ordered from the ACS, and can be downloaded from the Internet; see any current masthead page for ordering information and Internet access instructions.

JA950126+